Neurochemical Research (2019) 44:347–356
https://doi.org/10.1007/s11064-018-2682-9

ORIGINAL PAPER

Sevoflurane Postconditioning Inhibits Autophagy Through Activation of the Extracellular Signal-Regulated Kinase Cascade, Alleviating Hypoxic-Ischemic Brain Injury in Neonatal Rats

Shuo Wang[1] · Hang Xue[1] · Ying Xu[1] · Jiayuan Niu[1] · Ping Zhao[1]

Received: 16 January 2018 / Revised: 8 November 2018 / Accepted: 13 November 2018 / Published online: 20 November 2018

Abstract

Hypoxic-ischemic brain injury (HIBI) in neonates is one of the major contributors of newborn death and cognitive impairment. Numerous animal studies have demonstrated that autophagy is substantially increased in HIBI and that sevoflurane postconditioning (SPC) can attenuate HIBI. However, if SPC-induced neuroprotection inhibits autophagy in HIBI remains unknown. To investigate if cerebral protection induced by SPC is related to decreased autophagy in the setting of HIBI. Postnatal rats at day 7 (P7) were randomly assigned to 7 different groups: Sham, HIBI, SPC–HIBI, HIBI + rapamycin, SPC–HIBI + rapamycin, HIBI + p-extracellular signal-regulated kinase (p-ERK) inhibitor, and SPC–HIBI + p-ERK inhibitor. To induce HIBI, neonatal rats underwent left common carotid artery ligation, followed by 2 h of hypoxia (8% O_2). Rats in the SPC groups were treated with 1 minimum alveolar concentration ([MAC], 2.4%) SPC for 30 min after HIBI induction. Markers of autophagy and expression of ERK cascade components were measured in the rat brains after 24 h. Spatial learning and memory function were examined 29–34 days after administration of an autophagy agonist or a p-ERK inhibitor. The expression of microtubule-associated proteins 1A/1B, light chain 3B II (LC3-II) and tuberous sclerosis complex 2 (TSC2) were decreased in the SPC–HIBI group compared to the HIBI group. Expression of the p62 sequestosome 1 (P62/SQSTM1) protein, p-ERK/ERK, phospho-mammalian target of rapamycin (p-mTOR) and phospho-p70S6 were increased in SPC–HIBI group. Rats within the SPC–HIBI groups that also received the p-ERK inhibitor or autophagy inhibitor demonstrated reduced cross platform times and increased escape latency. Approximately 30 min of 2.4% SPC treatment in the P7 rat HIBI model attenuated excessive autophagy in the brain by elevating the ERK cascade. This finding provides additional insight into HIBI and identifies new targets for therapeutic approaches to treat HIBI.

Keywords Hypoxic-ischemic brain injury (HIBI) · Cognitive and memory impairment · Sevoflurane postconditioning (SPC) · Neuroprotection · Autophagy · ERK cascade

Abbreviations

HIBI	Hypoxic-ischemic brain injury
SPC	Sevoflurane postconditioning
ERK	Extracellular signal-regulated kinase
ERKI	ERK inhibitor

Introduction

Perinatal asphyxia is one of the major causes of newborn mortality and life-long neurodevelopmental disabilities [1]. Pathogenesis of perinatal asphyxia can be attributed to placental abruption, maternal infection, and umbilical cord prolapse, which induces hypoxia and ischemia in the central nervous system leading to hypoxic-ischemic brain injury (HIBI) [2]. During the first week of life in newborns, 20% of HIBI cases are fatal, and 50% of survivors develop life-long sequelae such as cognitive and memory impairments, cerebral palsy, and epilepsy [3, 4].

To date, the only clinically approved therapy for HIBI is moderate hypothermia [5, 6]. Several studies are currently investigating new HIBI treatments, such as administration of autologous cord blood cells intravenously [7], erythropoietin

✉ Ping Zhao
zhaoping_sj@163.com

[1] Department of Anesthesiology, Shengjing Hospital, China Medical University, Shenyang 110004, People's Republic of China

support, and sevoflurane postconditioning (SPC). Since neuronal cell death is a major contributor of HIBI sequelae, these therapies seek to prevent neuronal cell death. Morphological studies have identified three main types of cell death in HIBI; type 1 (apoptosis), type 2 (autophagic death), and type 3 (necrotic cell death) [8]. Several studies have focused on the role of sevoflurane postconditioning in alleviating HIBI by inhibition of necrotic cell death [9–11], however the effect of SPC on autophagic cell death in HIBI remains unknown.

Autophagy is a catabolic process essential to the proteasome pathway. However, in specific cases such as HIBI, overactive autophagy is deleterious due to its contribution to cell death. Pretreatment of neonatal rats with 3-methyladenine (3-MA), an autophagy inhibitor, significantly attenuated HIBI [12]. Besides the autophagic inhibitor, mTOR, acting downstream of the ERK cascade, can inhibit autophagy by preventing p-ULK1 activation [13]. ERK cascade plays a crucial role in multiple cellular processes including cell proliferation, differentiation, adhesion, migration and survival [14]. It has been shown that the ERK cascade has a neuroprotective role in HIBI [15], although the effect of the ERK cascade in SPC–HIBI remains to be clarified.

In this study, the involvement of autophagy and the ERK cascade in SPC-treated HIBI neonatal rats was investigated. The results of this study indicate that SPC treatment inhibits autophagy through activation of the ERK cascade to alleviate hypoxic-ischemic brain injury.

Materials and Methods

Animals

The animal studies were conducted during the synapse formation period of rat development, which occurs in postnatal development at day 7 (P7), equivalent to the period from late pregnancy to three years after birth in human babies [16]. All animal experiments were carried out in accordance with the National Institute of Health Guideline for the Care and Use of Laboratory Animals. Formal approval to conduct the experiments described was obtained from the animal review board of Shengjing Hospital, China Medical University.

Neonatal HIBI Model and Drug Administration

The HIBI model was used as previously described [17]. Briefly, postnatal Sprague–Dawley (SD) rats at day 7 (P7) (Laboratory of Shengjing Hospital, China Medical University; male/female ratio, 1:1) were sexed according to the distance between the reproductive organs and the anus. Cotton covered with sevoflurane was placed into a transparent plastic pipe and the head of the rats were placed into the pipe for anesthesia for approximately 20 s. Rats were then subjected to permanent double ligation of the left common carotid artery using 7–0 surgical silk and the artery was cut between two ligations. Every surgical operation was completed within 5 min. The rats were allowed to wake naturally and were returned to cages containing the mothers for 2 h. Rats were then put into an acrylic chamber for anesthesia with two connecting ducts on opposite sides of the chamber. One duct was connected to a sevoflurane vaporizer for ventilation, while the other duct transported the gas samples out of the chamber to a monitor. In the Sham group, the chamber was ventilated with 30% O_2 and 70% N_2 at a flow rate of 2 L/min for 2 h. In the HIBI group, the chamber was ventilated with 8% O_2 and 92% N_2 at a flow rate of 2 L/min for 2 h. SPC was established immediately after HIBI: rats inhaled 2.4% sevoflurane (1MAC) in a chamber with an atmosphere of 30% O_2, 70% N_2 at a flow rate of 2 L/min for 30 min. The chamber temperature was maintained at 37 °C using a heating pool. Drug administration: rats were anesthetized and placed in a stereotaxic frame. Rapamycin (RAP, 5 μg in 5 μL 0.1% DMSO; Selleck S1093) or p-ERK inhibitor (SCH772984 5 μg in 5 μL 0.1% DMSO; Selleck S7101) was injected into left lateral ventricle using a 5 μL Hamilton syringe exactly 30 min before HIBI. Rats in the treatment groups that did not receive rapamycin or p-ERK inhibitor received 0.1% DMSO alone.

Study Groups

A total of 150 P7 rats weighing 12–16 g were selected from 20 pregnant rats, and randomly assigned to groups using a random number table method. In total, 110 neonatal rats were analyzed with a mortality rate of 27% after HIBI treatment.

Thirty-five P7 SD rats were used for western blot coming from the groups as follows: Sham (n = 5), HIBI (n = 5), SPC–HIBI (n = 5), HIBI + rapamycin (n = 5), SPC–HIBI + rapamycin (n = 5), HIBI + p-ERKI (n = 5), and SPC–HIBI + p-ERKI (n = 5).

Twenty-five P7 SD rats were used for Immunohistochemistry coming from the groups as follows: Sham (n = 5), HIBI (n = 5), SPC–HIBI (n = 5), HIBI + p-ERKI (n = 5), and SPC–HIBI + p-ERKI (n = 5).

Fifty P7 SD rats were used in Suspension tests and Morris water maze (described below) coming from the groups as follows; Sham (n = 10), HIBI (n = 10), SPC–HIBI (n = 10), SPC–HIBI + rapamycin (n = 10), and SPC–HIBI + p-ERKI (n = 10).

Western Blot Analysis

Cotton covered with sevoflurane was placed into a transparent plastic pipe. The rat's head was then placed in for

anesthesia for approximately 20 s. Twenty-four hours after treatment, the left cerebral hippocampus from each group (n = 5 per group) was collected then placed on the ice. Supernatant total proteins were isolated after the addition of radio-immunoprecipitation assay agent (Beyotime, Haimen City, China). Protein concentrations were determined using a BCA kit. Samples (60 μg protein) were separated onto 12.5% SDS–polyacrylamide gels and transferred to a nitrocellulose membrane. After blocked with 5% non-fat milk, the membrane was incubated with the primary antibody overnight at 4 °C. The primary antibodies were: anti-β-actin (1:2000, Cell Signaling Technology, #3700), anti-LC3B (1:1000, polyclonal; Cell Signaling Technology, 2775S), anti-p62/SQSTM1 (1:1000, polyclonal; Cell Signaling Technology, 5114), anti-p44/42 MAPK (1:1000, monoclonal; Cell Signaling Technology, 4695P), anti-p-p44/42 MAPK (1:1000, monoclonal; Cell Signaling Technology, 4370P), anti-TSC2 (1:1000, monoclonal; Cell Signaling Technology, 4308S), anti-p-mTOR (1:1000, polyclonal; Cell Signaling Technology, 2971S), and anti-p-p70S6 (1:1000, monoclonal; Cell Signaling Technology, 9234S). The blots were then incubated with a horseradish peroxidase-conjugated secondary antibody at room temperature for 1 h. The protein blots were detected using enhanced chemiluminescence detection reagents (Thermo Scientific, Waltham, MA, USA). Protein band volumes were quantified by densitometry using Image Quant 5.0 Windows NT software (Molecular Dynamics, Sunnyvale, CA, USA). Blots were analyzed using the Gelpro32 (Media Cybernetics, USA). Data were normalized to β-actin as an internal control during the western blot analysis.

Immunohistochemistry

Following the anesthetic procedure mentioned above, the right atrial appendage of the rat heart was cut open and perfused with 4% formalin. The brain was then prepared for immunohistochemistry as follows. Briefly, the brains of rats (n = 5, per group) were first immersed in 4% paraformaldehyde (PFA) at 4 °C for 24 h, then embedded in paraffin wax after dehydration in graded ethanol. The tissue blocks were then sliced at 2.5 μm thickness using a paraffin slicer and paraffin sections were stored at room temperature until use. Each brain was serially sliced and 3 comparable brain slices were selected for LC3B staining. Tissue sections were incubated with primary antibody anti-LC3B (1:500, polyclonal; Cell Signaling Technology, 2775S) at 4 °C for 12 h in a humidified chamber. After three times of 5 min rinses in phosphate buffered saline (PBS), the sections were incubated with peroxidase-conjugated secondary antibody (no dilution, ZSGB-BIO, SP-9001). Diaminobenzidine (DAB) was applied for chromogenic staining. The nuclei were stained with hematoxylin (ZSGB-BIO, ZLI-9610). Finally, the sections were photographed with Nikon C1 microscope by an investigator blinded to the experimental intervention and groups. Each brain section of LC3B staining was photographed by at least 2 random fields of view and OD value was quantified using NIS-Elements AR Analysis 4.50.00 software. The LC3B positive cells were counted in a random reticle (approximately 0.01 mm^2) at × 400 magnification. Average values of three determinations were used to calculate the autophagic quantities.

Suspension Test

Suspension tests were performed to test motor outcomes once per day on day 21 to day 28 post HIBI. Rats (n = 10, per group) were forced to hold on to a 0.6-cm-wide plastic level, 45 cm above the ground, with their anterior limbs. The test was completed when the rat fell down, or when the suspending time reached 60 s, or when the rats' posterior limbs caught the level [12].

Morris Water Maze

The Morris water maze was used on day 29 to day 34 post HIBI to test spatial learning and memory (n = 10, per group). As described previously [12], the MWM was performed in a circular pool with black walls (diameter: 160 cm, depth: 60 cm). The pool was filled with 30-cm-deep warm water at 20 °C. An escape platform (diameter: 12 cm) was located 1.5 cm below the surface of water and at the center of the target quadrant. Probe trial sessions began at 8:00 am for 5 days and were conducted four times (once per quadrant) daily with 30 min rest time. Rats were put into the water to search for the hidden platform from four quadrants facing the pool wall. The duration spent on finding the platform (escape latency) was within 90 s. If the rat was not able to find the platform within 90 s, it was guided towards the platform and the escape latency was recorded as 90 s. After each trail, rats were made to stand on the platform for 20 s. During spatial probe test, rats were permitted to swim for 90 s freely after the platform was taken away from the maze. The entire process of MWM experiment was recorded by a camera located above the pool and analyzed using image analysis software (Shanghai Mobiledatum Ltd, China).

Statistical Analysis

The data were analyzed using Bartlett's test for equal variances and Shapiro–Wilk test for normality. Parametric data of the three groups was compared using one-way analysis of variance (ANOVA) followed by the Student–Newman–Keuls post hoc test, and nonparametric data of three groups were compared by the Kruskal–Wallis with Dunn's Multiple comparison test. The data of escape latency in the Morris water

maze test were analyzed using a repeated ANOVA. The spatial probe test data were analyzed using Kruskal–Wallis with Dunn's Multiple comparison test. All data were analyzed with GraphPad Prism 5.0 software or SPSS 20.0 software. Differences were considered to be statistically significant if $P < 0.05$. Data are presented as mean ± standard deviation (SD).

Results

HIBI Over-Activates Autophagy

In a previous study conducted in our laboratory, autophagy overactivation was found to be involved in HIBI in neonatal rats [12]. To further verify the autophagic activity in the setting of HIBI, the hippocampus of neonatal rats was examined using transmission electron microscope (TEM), which is considered the 'gold standard' for detecting the autophagic process. TEM revealed the presence of double-membrane cytoplasmic content containing vacuolar structures in the cytoplasm of neurons, confirming the formation of autophagosomes and autolysosomes (Fig. 1a).

SPC–HIBI Down-Regulates Over-Activated Autophagy

To study the neuroprotective mechanism of sevoflurane postconditioning (SPC) in HIBI, pivotal autophagic proteins including LC3BII and P62/SQSTM1 were examined 24 h after SPC–HIBI (Fig. 1). LC3 has two forms: LC3 I and LC3 II. When autophagy is initiated, LC3 II is formed by conjugation of LC3 I with phosphatidylethanolamine. Since the expression of LC3 I is quite abundant in brain tissue [18], we measured the expression of LC3 by detecting LC3B II compared to β-actin instead of the ratio of LC3 II/LC3 I and P62/SQSTM1, which is specially degraded in autolysosomes to detect intact autophagic flux. Decreased expression of LC3B II and increased expression of P62 were observed in the SPC–HIBI group compared to the HIBI group (Fig. 1b, HIBI vs. Sham: LC3B II: $P < 0.01$; P62: $P < 0.0001$; HIBI vs. SPC–HIBI: LC3B II: $P < 0.01$; P62: $P < 0.01$). Immunoperoxidase labeling of LC3B II showed reduced LC3B II in the SPC–HIBI group compared to the HIBI group (Fig. 1c, HIBI vs. Sham: LC3B II: $P < 0.0001$; HIBI vs. SPC–HIBI: LC3B II: $P < 0.0001$). To further verify the down-regulation of overactivated autophagy in SPC–HIBI, P7 rats were injected with rapamycin, an inducer of autophagy, intracerebroventricularly 30 min prior to HIBI treatment. Unlike the HIBI + rapamycin group, attenuated LC3B II expression and elevated P62/SQSTM1 expression were found in the SPC–HIBI + rapamycin group. No statistical

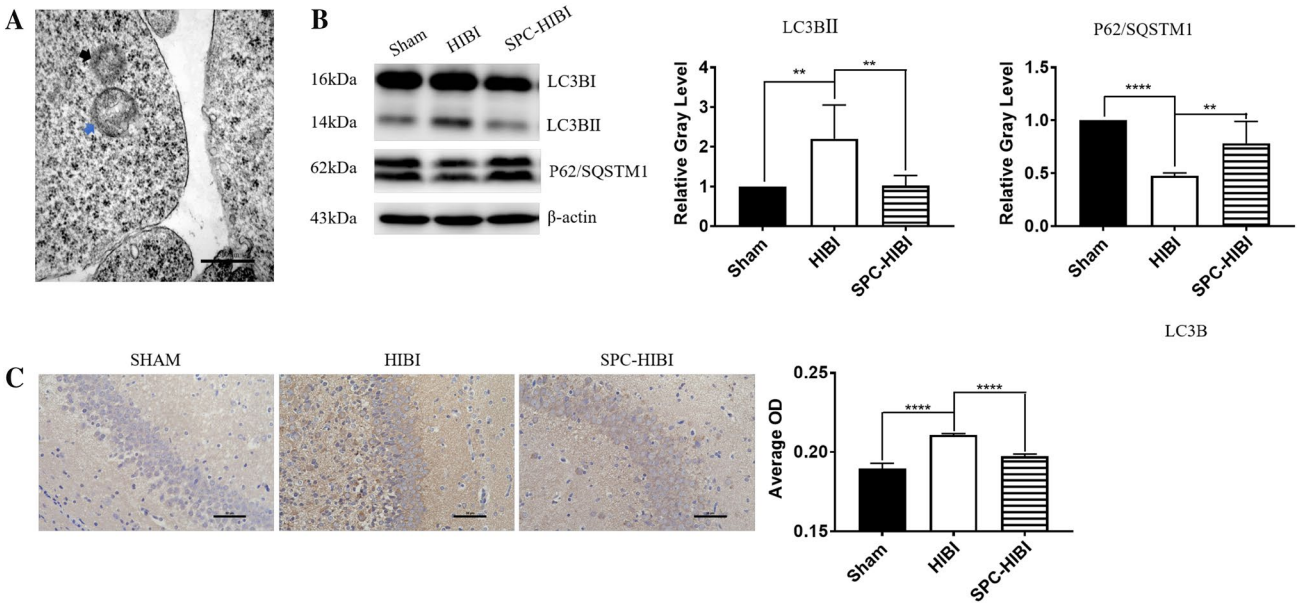

Fig. 1 HIBI upregulated autophagy and SPC treatment in the context of HIBI down-regulated autophagy in the hippocampus. Effects of HIBI on autophagy in TEM scan. Autophagosome (blue arrow head in **a**) and autolysosome (black arrow head in **a**) were observed after HIBI. Scale bar = 500 nm. Thirty minutes of 2.4% SPC–HIBI decreased expressions of LC3BII and increased the expression of P62 at the 24th h (**b, c**). Values are presented as mean ± SD, $n = 5$; $^{**}P < 0.01$, $^{****}P < 0.0001$. One-way ANOVA with Newman–Keuls post hoc test or Kruskal–Wallis with Dunn's Multiple comparison test was used for data analysis. (Color figure online)

difference in the expression of LC3B II or P62/SQSTM1 was observed between the HIBI and SPC–HIBI + rapamycin groups (Fig. 2, HIBI vs. HIBI + rapamycin: LC3B II: $P < 0.01$; P62: $P < 0.0001$; HIBI + rapamycin vs. SPC–HIBI + rapamycin: LC3B II: $P < 0.05$; P62: $P < 0.05$; HIBI vs. SPC–HIBI + rapamycin: LC3B II: $P > 0.05$; P62: $P > 0.05$; SPC–HIBI vs. SPC–HIBI + rapamycin: LC3B II: $P < 0.01$; P62: $P < 0.05$). Together, these results indicated that SPC treatment down-regulated overactivated autophagy during HIBI.

Down-Regulation of Over-Activated Autophagy in SPC–HIBI Involves the ERK Cascade

In the HIBI model, SPC treatment attenuated overactivated autophagy, however, the mechanism by which this occurred was unclear. Twenty-four hours after HIBI there was a reduction in expression of p-ERK, p-mTOR and p-p70S6 and enhanced TSC2 expression by western blot in the HIBI group compared to Sham rats (Fig. 3, HIBI vs. Sham: p-ERK: $P < 0.001$; TSC2: $P < 0.05$; p-mTOR: $P < 0.05$; p-p70S6: $P < 0.001$). In contrast, SPC treatment resulted in prominent p-ERK, p-mTOR, and p-p70S6 up-regulation as well as TSC2 down-regulation in the HIBI model (Fig. 3, SPC–HIBI vs. HIBI: p-ERK: $P < 0.001$; TSC2: $P < 0.05$; p-mTOR: $P < 0.05$; p-p70S6: $P < 0.05$;). To verify involvement of the ERK pathway, SCH772984, a p-ERK inhibitor (p-ERKI), was injected intracerebroventricularly into P7 rats 30 min prior to HIBI. SCH772984 suppressed the ERK cascade as revealed by reduced p-ERK, p-mTOR, p-p70S6 and elevated TSC2 expression. Inhibition of p-ERK further augmented autophagy flux in HIBI. The inhibitory effect of SPC on autophagy activation was significantly abolished by p-ERKI treatment, as indicated by increased LC3B II levels (Fig. 4, HIBI vs. HIBI + p-ERKI: p-ERK: $P < 0.05$; TSC2: $P < 0.01$; p-mTOR: $P < 0.05$; p-p70S6: $P < 0.01$; LC3B II: $P < 0.0001$; HIBI + p-ERKI vs. SPC–HIBI + p-ERKI: p-ERK: $P < 0.05$; TSC2: $P < 0.001$; p-mTOR: $P < 0.05$; p-p70S6: $P < 0.01$; LC3B II: $P < 0.0001$; HIBI vs. SPC–HIBI + p-ERKI: p-ERK: $P > 0.05$; TSC2: $P > 0.05$; p-mTOR: $P > 0.05$; p-p70S6: $P > 0.05$; LC3B II: $P > 0.05$;). Together, these results indicate that SPC treatment down-regulated overactivated autophagy through stimulation of the ERK cascade in HIBI.

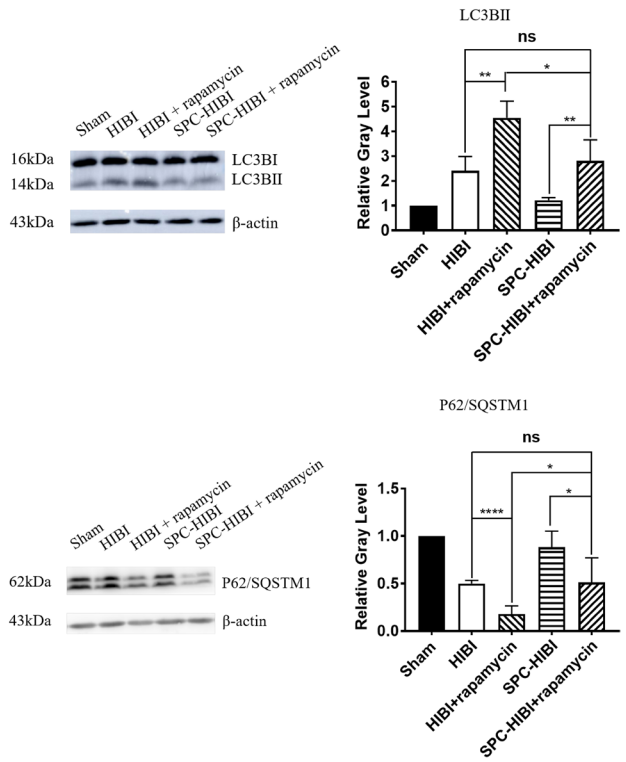

Fig. 2 Autophagy agonist attenuated the down-regulation of autophagy caused by SPC–HIBI in the hippocampus. P7 rats were pretreated with rapamycin 30 min before HIBI and autophagy was evaluated by LC3BII and p62. Values are presented as mean ± SD, $n = 5$; $^{*}P < 0.05$, $^{**}P < 0.01$, $^{****}P < 0.0001$. One-way ANOVA with Newman–Keuls post hoc test or Kruskal–Wallis with Dunn's Multiple comparison test was used for data analysis

Activation of Autophagy and Inhibition of ERK Cascade Attenuated the Improvement of Learning and Memory Caused by SPC–HIBI in P7 Rats

One of the most detrimental long-term effects of HIBI is impairment of learning and memory. A large body of evidence has demonstrated that SPC can improve learning and memory abilities after HIBI [19, 20]. Therefore, the role of autophagy and the ERK cascade in the improvement of learning and memory caused by SPC treatment during HIBI was also investigated. Learning and cognition were tested using the Morris water maze (MWM) on day 29 to day 34 after HIBI. No motor impairment was observed between the groups (Fig. 5). A significant difference was shown between groups during the learning phase which is the length of time using two-way ANOVA analysis (group: $P < 0.0001$; time: $P < 0.0001$). Consistent with previous findings, rats of the SPC–HIBI group reached the platform in a shorter amount of time compared to the HIBI group from the second day of training. Rapamycin or p-ERKI treatment dramatically increased the escape latency after SPC–HIBI. Therefore, no significant difference was found between the SPC–HIBI + rapamycin group, the SPC–HIBI + p-ERKI group and the HIBI group (Fig. 6a). In the spatial probe test, rats from the SPC–HIBI group made more passes across the platform than rats from the HIBI group (Fig. 6b, $P < 0.001$), the SPC–HIBI + rapamycin group (Fig. 6b, $P < 0.001$) and the SPC–HIBI + p-ERKI group (Fig. 6b, $P < 0.001$). No difference was detected between the SPC–HIBI + rapamycin group, the SPC–HIBI + p-ERKI group and the HIBI group.

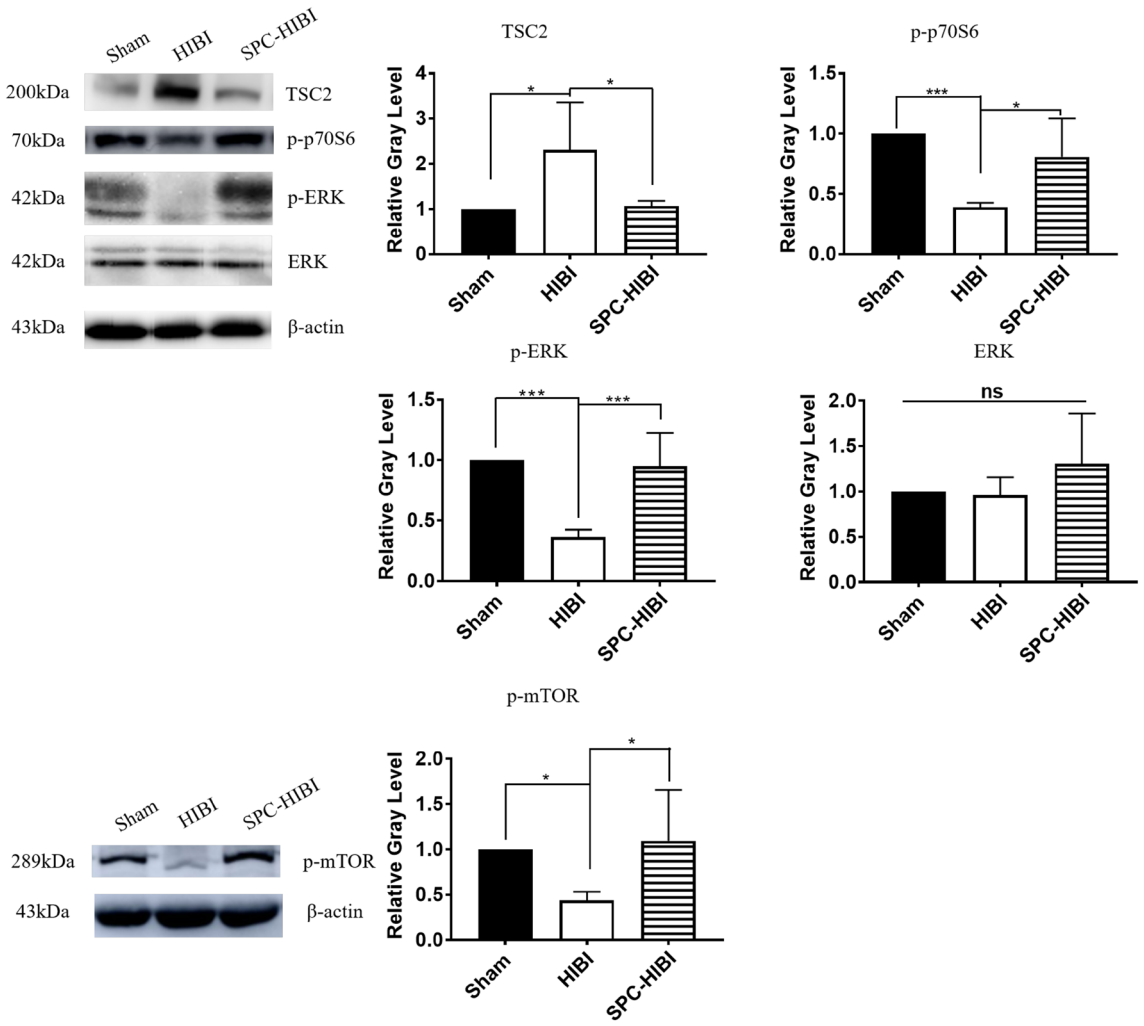

Fig. 3 SPC–HIBI upregulated the ERK cascade. SPC–HIBI upregulated p-ERK/ERK, p-mTOR and p-p70S6 expression and downregulated TSC2 expression at 24 h post HIBI. Values are presented as mean ± SD, $n = 5$; $^{*}P < 0.05$, $^{***}P < 0.001$, ns $P > 0.05$. One-way ANOVA with Newman–Keuls post hoc test or Kruskal–Wallis with Dunn's Multiple comparison test was used for data analysis

Discussion

In the last few years, intrapartum-related neonatal deaths have been the 5th most common cause of death among children under 5 years old [21]. Perinatal asphyxia, which contributes to HIBI, has an incidence of 1–6 per 1000 live births with a mortality rate up to 20%. Approximately 50% of survivors suffer from neuropsychological sequelae of immediate or delayed onset, while 25% of survivors show major neurological impairments [22].

To date, the only clinically approved therapy for HIBI is moderate hypothermia, however numerous studies have investigated alternative therapies including intravenous administration of autologous cord blood cells [7], erythropoietin support and SPC. Sevoflurane, an effective inhalational anesthetic, has been reported to play a protective role in neuronal HIBI by inhibiting apoptosis and necrosis [23].

In addition to apoptosis and necrosis, autophagy has been found to be over-activated in HIBI [12, 24–27]. Autophagy is a complex molecular process that plays an important role in physiological and vital functions including cellular homeostasis, cell growth and differentiation during the developmental period [28]. Whilst a basal level of autophagy is essential for the homeostasis of cells [2], the induction of autophagy can also result in negative effects on cellular function, depending on its level of activation. Recently, it has been reported that excessive autophagy is possibly involved in neuronal death following cerebral ischemia [29–32]. In cases of HIBI, over-activated autophagy can result in neuronal death. Puyal et al. demonstrated that pre-treatment, as well as, post-treatment of 3-MA, an inhibitor of autophagy, provided a strong neuroprotective effect against HIBI [33, 34]. Using genetic methodologies, including neuron-specific knockout of Atg7 [32] or knockdown of Beclin1, Koike et al.

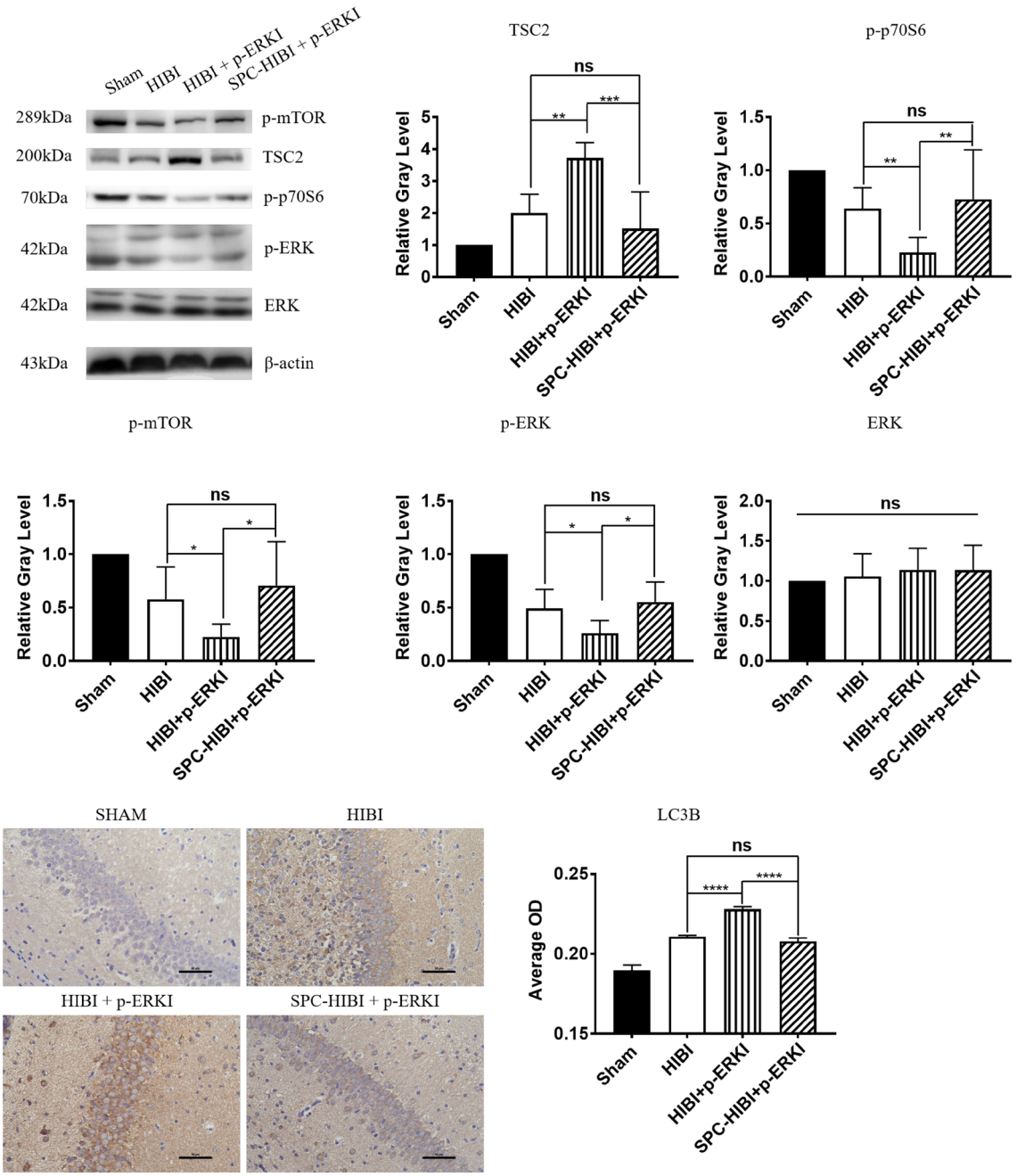

Fig. 4 p-ERK inhibitor attenuated the upregulation of ERK cascade and down-regulation of autophagy caused by SPC–HIBI in the hippocampus. P7 rats were pretreated with SCH772984 30 min before HIBI and the ERK cascade was evaluated by examining p-ERK/ERK, p-mTOR, p-p70S6 and TSC2 expression levels. Values are presented as mean ± SD, $n = 5$; $^{*}P < 0.05$, $^{**}P < 0.01$, $^{***}P < 0.001$, ns $P > 0.05$. One-way ANOVA with Newman–Keuls post hoc test or Kruskal–Wallis with Dunn's Multiple comparison test was used for data analysis

and Ginet et al. revealed a strong neuroprotective effect by inhibiting autophagy [26]. In the present study, SPC treatment alleviated HIBI by inhibiting autophagy in neonatal rats. In addition, SPC significantly decreased expression of LC3B II and increased expression of P62, compared to the no treatment HIBI group, indicating neuroprotection by SPC treatment was through inhibition of autophagy. The most commonly examined autophagy-related protein, LC3, is involved in phagophore formation, elongation and closure [35]. In addition to LC3, SQSTM1/P62 can also be used as autophagic protein markers. The SQSTM1 protein serves as a link between LC3 and ubiquitinated substrates. Both

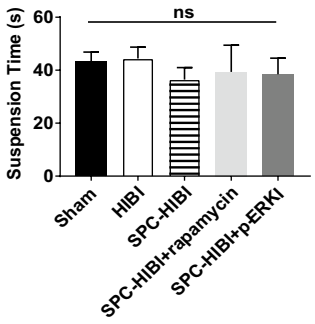

Fig. 5 Suspension test was performed before MWM on day 21 to day 28 (n = 10/group). No difference of motor function was found between groups. Values are presented with mean ± SD

SQSTM1 and SQSTM1-bound polyubiquitinated proteins become incorporated into the completed autophagosome and are degraded in autolysosomes, thus serving as a marker of autophagic degradation [36]. Here we demonstrated that in the HIBI group, LC3B II accumulation and P62 reduction indicated unobstructed autophagic flux and enhanced autophagic degradation within hippocampal tissue. In addition, the use of rapamycin to activate autophagy reduced the protective effect of sevoflurane on HIBI further demonstrating that sevoflurane alleviates HIBI by inhibiting autophagy.

The ERK cascade promotes cell survival by effecting growth factor action, cellular differentiation and proliferation [37]. The gene target downstream of the ERK cascade, mTOR, includes both mTORC1 and mTORC2. In this study, we examined mTORC1 as it has been shown that mTORC1 negatively regulates autophagy through coordinated phosphorylation of ULK1. Rapamycin can activate autophagy by disrupting mTORC1 dimerization and its integrity. Furthermore, TSC2, located upstream of mTORC1 in the ERK cascade, can negatively regulate mTORC1 through small molecule GTP enzyme Rheb [38]. Kovács et al. [37] and Kim et al. [39] have demonstrated that activation of the ERK cascade mitigates HIBI. In this study, SPC treatment augmented the ERK cascade thus reducing autophagy activation, as indicated by up-regulation of p-ERK, p-mTOR, p-p70s6, P62 and down-regulation of TSC2 and LC3B II. Treatment with the p-ERK inhibitor, SCH772984, blocked the response of ERK to SPC, eliminating the beneficial effects of SPC on HIBI. These results support the notion that SPC inhibits autophagy thereby alleviating HIBI through activation of the ERK cascade.

It has been shown that HIBI in neonates can impair learning and memory function during adolescence [4]. In this study, spatial learning and memory was tested using the MWM on day 29 to day 34 after HIBI. The protective effect of SPC treatment in the context of HIBI was significant in enhancing spatial learning (escape latency experiment) and spatial memory (platform crossing times experiment). Rapamycin or p-ERKI administration abolished the protective effect of SPC–HIBI, as shown by the increases in escape latency and decreases in the original platform crossing times.

This study includes several limitations; firstly, dynamic changes of autophagy over time after SPC–HIBI were not observed nor recorded and secondly the inhalation concentration of sevoflurane was maintained at a constant concentration (2.4%) rather than at a gradient of concentrations. Further studies on the protective effect of SPC treatment in the context of HIBI are necessary to eliminate these limitations. In addition, genetic methodologies, such as neuron-specific knockout of an autophagic gene, would be beneficial in further determining the neuroprotective role of SPC treatment by autophagy inhibition.

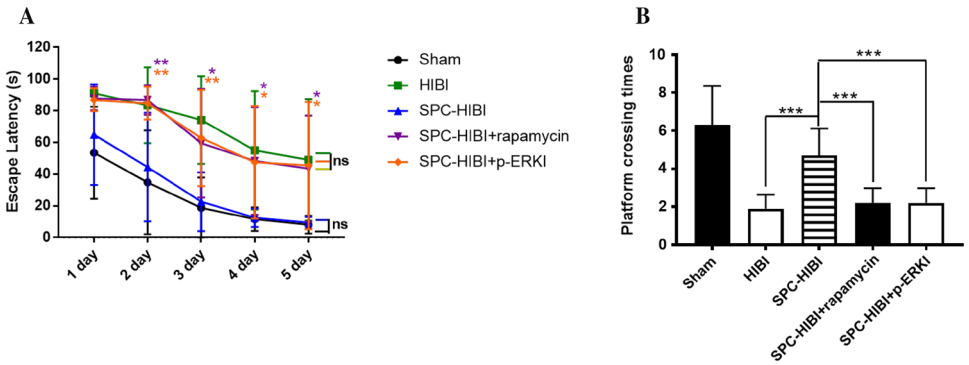

Fig. 6 Activation of autophagy and inhibition of ERK cascade attenuated the improvement of learning and memory caused by SPC–HIBI in P7 rats. Spatial cognitive performance was tested in the Morris water on day 29 to day 34. The behavioral tests were evaluated by escape latency (**a**) and times across the platform (**b**). Values are presented as mean ± SD, $n = 10$; $^{*}P < 0.05$, $^{**}P < 0.01$, $^{***}P < 0.001$, ns $P > 0.05$. The data of escape latency were analyzed using two-way ANOVA followed by Bonferroni posttest. The spatial probe test was performed at P34 and analyzed using Kruskal–Wallis with Dunn's Multiple comparison test

Conclusion

This study indicates that SPC inhibits autophagy thus alleviating HIBI through activation of the ERK cascade in neonatal rats. These findings provide new avenues of development for new therapeutic approaches against HIBI in neonatal rats, and potentially humans.

Author Contributions SW and PZ designed the experiments. SW, HX and PZ contributed to the planning of the work. SW performed all the experiments with the help of HX, YX and JN. HX, YX and JN participated in the data collection. SW, YX and JN analyzed and interpreted the results. SW wrote the manuscript with the help of YX. PZ supervised the project and revised the article.

Funding This study was supported by two grants from the National Natural Science Foundation of China (Nos. 81171782, 81671311), one grant from Science and Technology foundation of Liaoning province (No. 2015020467), one grant from the Outstanding Scientific Fund of Shengjing Hospital (No. 201708).

Compliance with Ethical Standards

Conflict of interest The authors declare that they have no conflict of interest.

Ethics Approval All animal experiments were carried out in accordance with the National Institute of Health Guideline for the Care and Use of Laboratory Animals. Formal approval to conduct the experiments described has been obtained from the animal review board of Shengjing Hospital, China Medical University.

References

1. Edwards A, Brocklehurst P, Gunn A, Halliday H, Juszczak E, Levene M, Strohm B, Thoresen M, Whitelaw A, Azzopardi D (2010) Neurological outcomes at 18 months of age after moderate hypothermia for perinatal hypoxic ischaemic encephalopathy: synthesis and meta-analysis of trial data. BMJ 340:c363
2. Descloux C, Ginet V, Clarke PG, Puyal J, Truttmann AC (2015) Neuronal death after perinatal cerebral hypoxia-ischemia: Focus on autophagy-mediated cell death. Int J Dev Neurosci 45:75–85. https://doi.org/10.1016/j.ijdevneu.2015.06.008
3. Okereafor A, Allsop J, Counsell SJ, Fitzpatrick J, Azzopardi D, Rutherford MA, Cowan FM (2008) Patterns of brain injury in neonates exposed to perinatal sentinel events. Pediatrics 121(5):906–914. https://doi.org/10.1542/peds.2007-0770
4. Vannucci SJ, Hagberg H (2004) Hypoxia-ischemia in the immature brain. J Exp Biol 207(Pt 18):3149–3154. https://doi.org/10.1242/jeb.01064
5. Stankowski JN, Gupta R (2011) Therapeutic targets for neuroprotection in acute ischemic stroke: lost in translation? Antioxid Redox Signal 14(10):1841–1851. https://doi.org/10.1089/ars.2010.3292
6. Yuan J (2009) Neuroprotective strategies targeting apoptotic and necrotic cell death for stroke. Apoptosis 14(4):469–477. https://doi.org/10.1007/s10495-008-0304-8
7. Cotten CM, Murtha AP, Goldberg RN, Grotegut CA, Smith PB, Goldstein RF, Fisher KA, Gustafson KE, Waters-Pick B, Swamy GK, Rattray B, Tan S, Kurtzberg J (2014) Feasibility of autologous cord blood cells for infants with hypoxic-ischemic encephalopathy. J Pediatr 164(5):973–979 e971. https://doi.org/10.1016/j.jpeds.2013.11.036
8. Puyal J, Ginet V, Clarke PG (2013) Multiple interacting cell death mechanisms in the mediation of excitotoxicity and ischemic brain damage: a challenge for neuroprotection. Prog Neurobiol 105:24–48. https://doi.org/10.1016/j.pneurobio.2013.03.002
9. Kim H, Kim E, Bae J, Lee K, Jeon Y, Hwang J, Lim Y, Min S, Park H (2017) Sevoflurane postconditioning reduces apoptosis by activating the JAK-STAT pathway after transient global cerebral ischemia in rats. J Neurosurg Anesthesiol 29(1):37–45
10. Wang H, Shi H, Yu Q, Chen J, Zhang F, Gao Y (2016) Sevoflurane preconditioning confers neuroprotection via anti-apoptosis effects. Acta Neurochir Suppl 121:55–61. https://doi.org/10.1007/978-3-319-18497-5_10
11. Hwang J, Jeon Y, Lim Y, Park H (2017) Sevoflurane postconditioning-induced anti-inflammation via inhibition of the toll-like receptor-4/nuclear factor Kappa B pathway contributes to neuroprotection against transient global cerebral ischemia in rats. Int J Mol Sci 18(11):2347
12. Xu Y, Tian Y, Tian Y, Li X, Zhao P (2016) Autophagy activation involved in hypoxic-ischemic brain injury induces cognitive and memory impairment in neonatal rats. J Neurochem 139(5):795–805. https://doi.org/10.1111/jnc.13851
13. Shang L, Chen S, Du F, Li S, Zhao L, Wang X (2011) Nutrient starvation elicits an acute autophagic response mediated by Ulk1 dephosphorylation and its subsequent dissociation from AMPK. Proc Natl Acad Sci USA 108(12):4788–4793. https://doi.org/10.1073/pnas.1100844108
14. von Kriegsheim A, Baiocchi D, Birtwistle M, Sumpton D, Bienvenut W, Morrice N, Yamada K, Lamond A, Kalna G, Orton R, Gilbert D, Kolch W (2009) Cell fate decisions are specified by the dynamic ERK interactome. Nat Cell Biol 11(12):1458–1464. https://doi.org/10.1038/ncb1994
15. Yuan JH, Pan F, Chen J, Chen CE, Xie DP, Jiang XZ, Guo SJ, Zhou J (2017) Neuroprotection by plumbagin involves BDNF-TrkB-PI3K/Akt and ERK1/2/JNK pathways in isoflurane-induced neonatal rats. J Pharm Pharmacol 69(7):896–906. https://doi.org/10.1111/jphp.12681
16. Jevtovic-Todorovic V, Hartman RE, Izumi Y, Benshoff ND, Dikranian K, Zorumski CF, Olney JW, Wozniak DF (2003) Early exposure to common anesthetic agents causes widespread neurodegeneration in the developing rat brain and persistent learning deficits. J Neurosci 23(3):876–882
17. Zhao P, Peng L, Li L, Xu X, Zuo Z (2007) Isoflurane preconditioning improves long-term neurologic outcome after hypoxic-ischemic brain injury in neonatal rats. Anesthesiology 107(6):963–970. https://doi.org/10.1097/01.anes.0000291447.21046.4d
18. Yang DS, Stavrides P, Mohan PS, Kaushik S, Kumar A, Ohno M, Schmidt SD, Wesson D, Bandyopadhyay U, Jiang Y, Pawlik M, Peterhoff CM, Yang AJ, Wilson DA, St George-Hyslop P, Westaway D, Mathews PM, Levy E, Cuervo AM, Nixon RA (2011) Reversal of autophagy dysfunction in the TgCRND8 mouse model of Alzheimer's disease ameliorates amyloid pathologies and memory deficits. Brain 134(Pt 1):258–277. https://doi.org/10.1093/brain/awq341
19. Hu X, Wang J, Zhang Q, Duan X, Chen Z, Zhang Y (2016) Postconditioning with sevoflurane ameliorates spatial learning and memory deficit after hemorrhage shock and resuscitation in rats. J Surg Res 206(2):307–315
20. Lai Z, Zhang L, Su J, Cai D, Xu Q (2016) Sevoflurane postconditioning improves long-term learning and memory of neonatal hypoxia-ischemia brain damage rats via the PI3K/Akt-mPTP pathway. Brain Res 1630:25–37

21. Lawn J, Bahl R, Bergstrom S, Bhutta Z, Darmstadt G, Ellis M, English M, Kurinczuk J, Lee A, Merialdi M, Mohamed M, Osrin D, Pattinson R, Paul V, Ramji S, Saugstad O, Sibley L, Singhal N, Wall S, Woods D, Wyatt J, Chan K, Rudan I (2011) Setting research priorities to reduce almost one million deaths from birth asphyxia by 2015. PLoS Med 8(1):e1000389
22. Fineschi V, Viola RV, La Russa R, Santurro A, Frati P (2017) A controversial medicolegal issue: timing the onset of perinatal hypoxic-ischemic brain injury. Mediators Inflamm 2017:6024959. https://doi.org/10.1155/2017/6024959
23. Wang Z, Ye Z, Huang G, Wang N, Wang E, Guo Q (2016) Sevoflurane post-conditioning enhanced hippocampal neuron resistance to global cerebral ischemia induced by cardiac arrest in rats through PI3K/Akt survival pathway. Front Cell Neurosci 10:271. https://doi.org/10.3389/fncel.2016.00271
24. Ginet V, Puyal J, Clarke PG, Truttmann AC (2009) Enhancement of autophagic flux after neonatal cerebral hypoxia-ischemia and its region-specific relationship to apoptotic mechanisms. Am J Pathol 175(5):1962–1974. https://doi.org/10.2353/ajpath.2009.090463
25. Piras A, Gianetto D, Conte D, Bosone A, Vercelli A (2011) Activation of autophagy in a rat model of retinal ischemia following high intraocular pressure. PLoS ONE 6(7):e22514. https://doi.org/10.1371/journal.pone.0022514
26. Ginet V, Spiehlmann A, Rummel C, Rudinskiy N, Grishchuk Y, Luthi-Carter R, Clarke PG, Truttmann AC, Puyal J (2014) Involvement of autophagy in hypoxic-excitotoxic neuronal death. Autophagy 10(5):846–860. https://doi.org/10.4161/auto.28264
27. Liu Y, Levine B (2015) Autosis and autophagic cell death: the dark side of autophagy. Cell Death Differ 22(3):367–376
28. Puyal J, Ginet V, Grishchuk Y, Truttmann AC, Clarke PG (2012) Neuronal autophagy as a mediator of life and death: contrasting roles in chronic neurodegenerative and acute neural disorders. Neuroscientist 18(3):224–236. https://doi.org/10.1177/1073858411404948
29. Zhu C, Wang X, Xu F, Bahr BA, Shibata M, Uchiyama Y, Hagberg H, Blomgren K (2005) The influence of age on apoptotic and other mechanisms of cell death after cerebral hypoxia-ischemia. Cell Death Differ 12(2):162–176. https://doi.org/10.1038/sj.cdd.4401545
30. Adhami F, Liao G, Morozov YM, Schloemer A, Schmithorst VJ, Lorenz JN, Dunn RS, Vorhees CV, Wills-Karp M, Degen JL, Davis RJ, Mizushima N, Rakic P, Dardzinski BJ, Holland SK, Sharp FR, Kuan CY (2006) Cerebral ischemia-hypoxia induces intravascular coagulation and autophagy. Am J Pathol 169(2):566–583. https://doi.org/10.2353/ajpath.2006.051066
31. Wen YD, Sheng R, Zhang LS, Han R, Zhang X, Zhang XD, Han F, Fukunaga K, Qin ZH (2008) Neuronal injury in rat model of permanent focal cerebral ischemia is associated with activation of autophagic and lysosomal pathways. Autophagy 4(6):762–769
32. Koike M, Shibata M, Tadakoshi M, Gotoh K, Komatsu M, Waguri S, Kawahara N, Kuida K, Nagata S, Kominami E, Tanaka K, Uchiyama Y (2008) Inhibition of autophagy prevents hippocampal pyramidal neuron death after hypoxic-ischemic injury. Am J Pathol 172(2):454–469. https://doi.org/10.2353/ajpath.2008.070876
33. Puyal J, Clarke P (2009) Targeting autophagy to prevent neonatal stroke damage. Autophagy 5(7):1060–1061
34. Puyal J, Vaslin A, Mottier V, Clarke P (2009) Postischemic treatment of neonatal cerebral ischemia should target autophagy. Ann Neurol 66(3):378–389
35. Weidberg H, Shvets E, Shpilka T, Shimron F, Shinder V, Elazar Z (2010) LC3 and GATE-16/GABARAP subfamilies are both essential yet act differently in autophagosome biogenesis. EMBO J 29(11):1792–1802. https://doi.org/10.1038/emboj.2010.74
36. Mizushima N, Yoshimori T (2007) How to interpret LC3 immunoblotting. Autophagy 3(6):542–545
37. Kovács V, Tóth-Szűki V, Németh J, Varga V, Remzső G, Domoki F (2018) Active forms of Akt and ERK are dominant in the cerebral cortex of newborn pigs that are unaffected by asphyxia. Life Sci 192:1–8
38. Egan D, Kim J, Shaw RJ, Guan KL (2011) The autophagy initiating kinase ULK1 is regulated via opposing phosphorylation by AMPK and mTOR. Autophagy 7(6):643–644
39. Kim SY, Cheon SY, Kim EJ, Lee JH, Kam EH, Kim JM, Park M, Koo BN (2017) Isoflurane postconditioning inhibits tPA-induced matrix metalloproteinases activation after hypoxic injury via low-density lipoprotein receptor-related protein and extracellular signal-regulated kinase pathway. Neurochem Res 42(5):1533–1542. https://doi.org/10.1007/s11064-017-2211-2